15TH IEA HEAT PUMP CONFERENCE
MAY 26–29, 2026 | HOFBURG
VIENNA 2026
DECARBONISATION THROUGH INNOVATION

Integration of High Temperature Heat Pumps in the Drying Process of Packaging Paper and Tissue

Afsaneh Norouzian[a, *], Sebastian Dickler[a], Isabel Kuperjans[a]

[a]Institute NOWUM-Energy, FH Aachen - University of Applied Sciences, Jülich 52428, Germany
{norouzian, dickler, kuperjans}@fh-aachen.de

Abstract

The paper drying process is highly energy intensive and contributes significantly to CO_2 emissions. Integrating high temperature heat pumps for waste heat recovery and electrifying this process, offers a pathway to reduce fossil fuel use in the paper industry.
This study evaluates the integration of a high temperature heat pump into two distinct drying methods: cylinder drying for packaging paper and Yankee cylinder drying for tissue. It aims to compare how high temperature heat pump integration affects each process in comparison to a conventional natural gas boiler. Key variables include refrigerant type, exhaust air (source) properties, steam (sink) properties, and system configurations. The simulation quantifies the coefficient of performance, and the reduction in final energy consumption per ton of paper in the dryer section. In addition, a pinch analysis estimates the maximum recoverable waste heat potential.
The best-performing model uses R601a in a high temperature heat pump with an internal heat exchanger, a turboexpander- coupled to a steam compressor to boost steam conditions to the dryer, and water injection to control steam superheating. In this case the total coefficient of performance reaches 2.8 for packaging paper drying and 1.9 for tissue drying, while the energy consumption per ton of paper (just the thermal energy for the drying section) falls by 68 % and 61.7 %, respectively, compared to a conventional natural gas boiler.
Pinch analysis of the packaging paper dryer shows that a drying section with high temperature heat pump integrated, can eliminate hot utility demand, shifting 885 kWh/t_{paper} of thermal demand to 293 kWh/t_{paper} of electricity, and cut unused waste heat by 54%.
The study demonstrates that heat pump integration can substantially improve energy efficiency in energy supply system for paper drying, with performance varying by paper grade and drying method.

Keywords: Waste heat recovery; High temperature heat pump; Refrigerant; Pinch analysis; Paper drying process

1. Introduction

To achieve global environmental protection targets, it is important to reduce the carbon footprint of energy-intensive industries such as paper production. According to the Confederation of European Paper Industries (CEPI), decarbonizing process heat, which accounts for around 70% of the energy consumed in paper mills for drying paper at 100-550 °C, should be a top priority for the EU Innovation Fund [1]. CEPI encourages support for a wide range of options for decarbonizing heat supply (e.g., waste heat recovery) [2]. The use of energy-saving technologies, especially in the paper drying process, such as the integration of auxiliary technologies like high temperature heat pumps (HTHPs), can reduce energy consumption while also reducing CO2 emissions from fuel combustion [3]. This approach is also in line with the general goal of the "Modellfabrik Papier" research cluster, which is to cut energy use in paper production by 80% [4].

1.1. High-Temperature Heat Pumps for Industrial Electrification

Compared with fuel-fired boilers, HTHP systems can deliver the same thermal duty at higher primary-energy efficiency by upgrading low-to-medium-temperature waste heat to usable steam.

Recent studies conclude that HTHPs are technically mature across multiple architectures (single-stage, cascade and hybrid/ mechanical vapor recompression (MVR)-assisted) and are already capable of producing process steam well above 120 °C for industrial service [5].

Another study [3], demonstrates the potential of HTHPs for industrial electrification by integrating a novel MVR system into a paper mill's steam network. Using a prototype piston compressor, the system efficiently generates steam at 180 °C, showcasing rapid start-up and stable operation with a pressure ratio of 3. Advanced control strategies, including adaptive feedforward and feedback mechanisms, enable safe, precise temperature regulation and effective condensate injection. The results of their research highlight the feasibility of retrofitting HTHPs into existing industrial infrastructure, supporting the transition to low-emission process heat.

[6] explores the integration of a cascade HTHP in a Northern Italy pulp and paper facility to enhance energy circularity by recovering heat from wastewater. The 1.3 MWth system supplies 120 °C heat for drying while cooling wastewater, yielding benefits such as reduced sludge volume, lower CO_2 emissions, and decreased auxiliary power demand. They concluded that despite the environmental gains, which have led to savings of up to 1989 tons/year CO_2, the economic analysis reveals negative net present value under current conditions, whether powered by a natural gas CHP unit or supplemented with a PV system. Their findings emphasize the critical role of incentives and heat pump coefficient of performance (COP) in achieving financial viability.

The design of an HTHP system for paper drying depends on the match between source and sink, as well as the required temperature rise. The choice of cycle and integration details, whether single-stage or cascaded layout, internal heat exchange, steam side compression, or hybridization with MVR, have a strong influence on COP and compressor discharge temperatures.

On the working fluid side, recent studies continue to show that R-1233zd(E) is attractive due to its favorable thermophysical properties, good efficieny at elevated condensation temperatures, and comparatively low GWP, although compromises in terms of volumetric capacity and flammability/toxicity limitations must also be considered. Meanwhile, new candidates are being investigated: fluorobenzene has shown promising performance in two-stage throttle cycles, achieving a COP of around 3.25 at a condensation temperature of 180 °C with a stroke of around 100 K, demonstrating pathways to high-quality steam without excessive efficiency losses [7].

From a system engineering perspective, successful integration into factories depends on HTHPs being designed to address process bottlenecks, exhaust air humidity and temperature, and condensate return conditions. Careful selection of source streams and control of superheating can prevent exergy destruction in the steam cycle [8]. As the electricity mix becomes more decarbonized, the emissions saving potential of HTHPs increases. Policy analysis suggests that industrial heat pumps in Europe could mobilize hundreds of TWh of currently unused waste and ambient heat if supported by clear market signals and investment frameworks (e.g., appropriate allocations and innovation financing) [8]. These findings are important for paper mills, as they concern both the technology at the site level (dimensioning, temperature increases, fluids) and the conditions for economic viability (electricity price structures, CO_2 costs, subsidy programs).

The study of [9] indicates that advanced HTHPs using low-GWP refrigerants can efficiently upgrade industrial waste heat, with the best configuration dictated by temperature lift. Evaluating eight cycles and nine refrigerants (all with an internal heat exchanger), it shows single-stage layouts suit ≤50 K lifts, while two-stage options, especially cascade/booster and extraction concepts, excel for ≥60 K lifts, dual heat sources, or high sink-glide demands, yielding large COP and volumetric heating-capacity gains over a reference cycle. Refrigerant screening highlights trade-offs: HC-601, HFO-1336mzz(Z) and R-514A tend to maximise COP but with lower volumetric heating capacity (VHC); HC-600/600a maximise VHC with small or negative COP changes; HCFO-1233zd(E) and HCFO-1224yd(Z) provide balanced performance. A cost comparison finds only around 9% difference relative to the reference configuration, and a total equivalent warming impact analysis suggests up to 68% lower equivalent CO_2 versus a natural-gas boiler. Overall, [9] supports HTHPs as technically and economically viable for electrifying medium-to-high-temperature process heat when carefully matched to source/sink conditions and working fluid.

The current findings indicate that HTHPs can replace a significant portion of the steam used in industrial applications while reducing final energy consumption and CO_2 emissions, especially if (i) conditions at the source/sink ensure moderate lift levels, (ii) cycles and fluids are selected for produce high-temperature steam, and (iii) the waste heat potential of the factory is fully optimized through integration [3].

In total, ongoing studies suggest that the targeted use of HTHPs in industry, once they are technically feasible for use at higher temperatures, can lead to significant energy savings and CO_2 reductions.

1.2. Research Objectives

Based on recent literature highlighting the role of HTHPs in the electrification of energy-intensive industries, and mostly based on the findings of [10], [11], this study focuses on design and benchmarking at the process level. It examines the integration of HTHPs in two example drying systems: (i) cylinder drying for packaging paper and (ii) Yankee cylinder drying for tissue, compared to a conventional natural gas boiler as a reference system. Main objectives are as follows:

- **Design and modelling:** Development of physics-based models (Self-developed Python models) of HTHPs integrated into each drying method, testing of an HTHP model with internal heat exchanger (IHX), turboexpander, and steam compression after the HTHP, and water injection to control the steam temperature suitable for our drying operation, while testing different refrigerants (focus on natural hydrocarbons and water).
- **Performance quantification:** For realistic source/sink conditions, compute coefficient of performance (COP), and specific final energy per ton of paper.
- **Waste-heat matching:** Use pinch analysis to estimate the maximum recoverable heat and control the integration of the heat pump into the exhaust air/condensate networks of the drying section. In this article, pinch analysis is performed only for the case of packaging paper and only for the drying section, while further details on the process are available.

This paper aims to answer following research questions:

- How can a HTHP be integrated into the dryer section of packaging paper and tissue machines, and what efficiency levels (COP, specific energy) can be achieved compared to a gas boiler?
- How do steam pressure and temperature requirements, which vary depending on the mill and grade, affect HTHP performance?
- Which refrigerants provide the best trade-off between COP and energy consumption for each drying method?
- According to the pinch analysis, what fraction of dryer-section waste heat is recovered by the HTHP and what fraction remains unused?

2. Method

This part presents three HTHPs system models to investigate the feasibility and performance benefits of integrating a HTHP into the drying section of the production process for packaging paper and tissue paper. Fig. 1 presents the baseline scenario for packaging paper, while Fig. 2 outlines the tissue base case scenario as defined in the study of [10]. In the packaging paper manufacturing sector, industrial paper machines mechanically dewater the paper and then dry it on steam-heated cylinder dryers. The paper is wrapped around several cylinders in sequence, whereby the water evaporates and the moist exhaust air is removed [12]. In European paper factories, approximately 70% of the total steam demand is accounted for by pressures below 5 bar [1]. For this assessment, a base scenario is defined based on various studies [1], [12], and process information from a paper mill in Germany.

In the base case for packaging paper, see Fig. 1, the drying section requires steam at a temperature of approximately 165 °C and a pressure of 3 bar, with a specific steam requirement of around 1.4 tons of steam per tons of paper. The selected setpoint of 165 °C is 15 K above the reference value in [1], to cover distribution losses. The steam is generated in a natural gas boiler with an estimated efficiency of 97%, resulting in a specific fuel consumption of 885 kWh per ton of paper. The steam condenses inside the cylinders and the condensate is returned to the boiler in a closed circuit. On the air flow side, outside air with a temperature of around 12 °C and a humidity of 70 % is preheated to 42 °C via a heat exchanger with the dryer exhaust air before it enters the hoods. The mixed exhaust air from all dryers exits at a temperature of approximately 58 °C and a humidity of 73%, carrying the latent heat from evaporation.

The information on the base scenario for tissue production comes from the study by [10] and is illustrated in Fig. 2. A modern tissue machine dries a mechanically dewatered web on a single large Yankee cylinder with high-speed hood impingement. Natural gas has two functions: burners heat the hood air to around 500 °C, and a boiler generates 17 bar saturated steam. The Yankee is fed with 9 bar saturated steam, pressure drops generate 8 bar blow-through steam, which is compressed back to 9 bar by a steam thermocompressor using the 17 bar of motive steam. The plant produces about 5 t/h of paper, evaporates 5.5 t/h of water, and the moist hood exhaust air leaves the hood at about 310 °C and, after heat recovery through heat exchangers, finally at 75 °C. The condensate is phase-separated and returned to the boiler, while fresh air replaces the removed moist air.

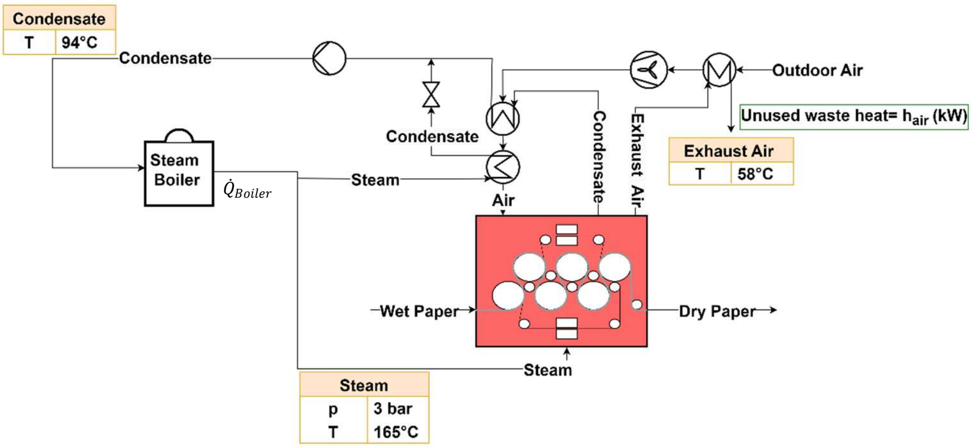

Figure 1. Base case scenario, packaging paper

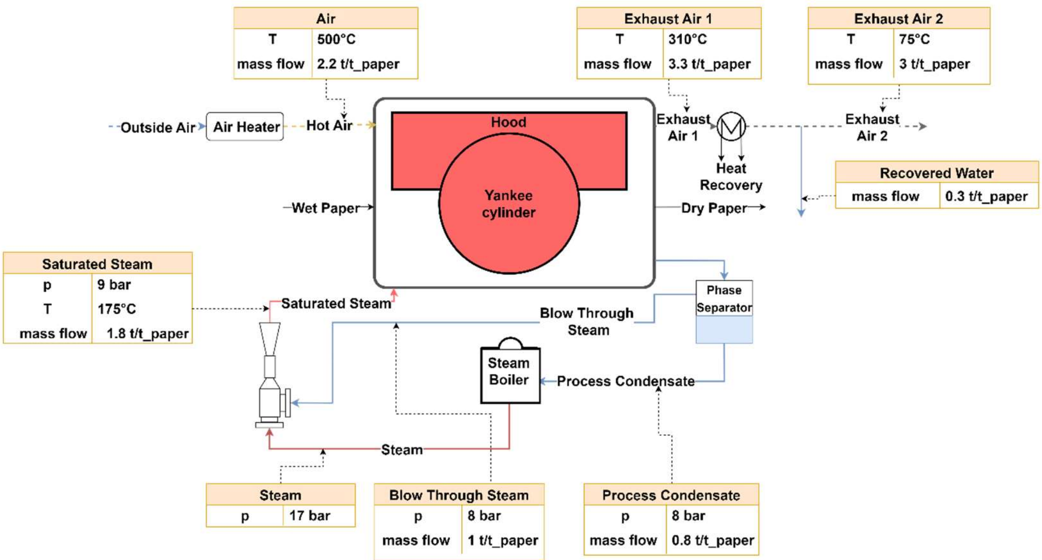

Figure 2. Base case scenario, tissue paper [10].

2.1. Configurations of High-Temperature Heat Pumps for the Base Cases

Three HTHP integration variants are evaluated: In the first proposed configuration (Fig. 3(a)), saturated low-pressure steam (1.3 bar, 107 °C) is generated by the single-stage heat pump, which is increased to dryer pressure by a mechanical steam compressor and reduced to 165 °C in the cylinders by controlled condensate injection. In the second configuration (Fig. 3(b)), the first layout is extended by an internal heat exchanger (IHX), which increases the liquid subcooling at the condenser outlet (while simultaneously increasing the suction superheat), thereby improving the overall efficiency of the cycle [13]. And in the last model (Fig. 3(c)), the throttle valve is replaced by a near-isentropic turboexpander, which recovers the expansion work, reduces the enthalpy of the refrigerant at the evaporator outlet, and reduces the compressor power. This devices described are characterized by an isentropic efficiency of approximately 59-65% and a work recovery of around 33-40%, resulting in a higher COP [14].

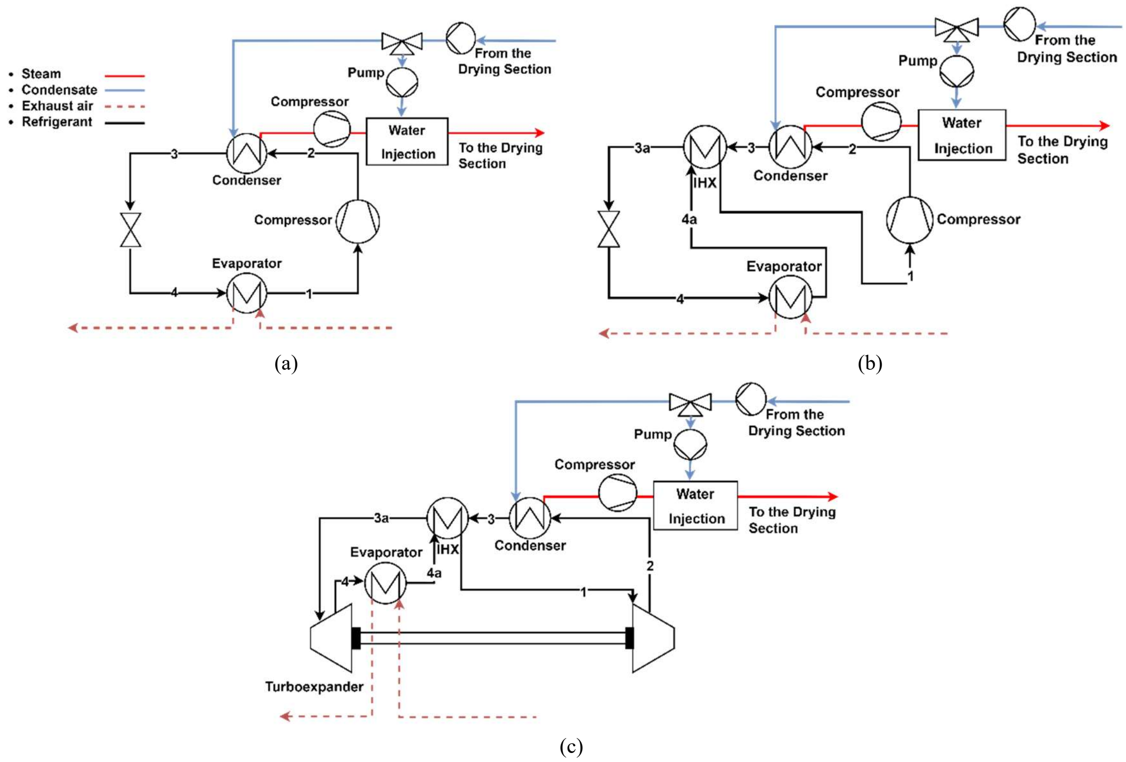

Figure 3. HTHP integration models: (a) one stage heat pump, and steam compressor; (b) one stage heat pump with IHX, and steam compressor; (c) one stage heat pump with IHX, turboexpander, and steam compressor after the heat pump

Figs. 4 and 5 demonstrate possible integrations of HTHP in paper machine dryers (Second proposed HTHP model is used for these illustrations): The exhaust air from the hood is utilized as a heat source in the evaporator. On the hot side, the condenser evaporates the return condensate to produce low-pressure saturated steam (107-120 °C), which is then mechanically compressed to the required dryer pressure, with condensate injection balancing the excess superheat before the cylinders. In the packaging and tissue cases, the HTHP replaces the steam boiler. In the tissue case (Fig. 5), a steam compressor replaces the thermocompressor, and the blow-through steam is recompressed after phase separation.

The thermocompressor is replaced because it requires higher pressure motive steam to entrain the 8 bar blow-through steam and compress it to Yankee pressure [10]. And in the HTHP scenario, there is no 17-bar motive steam available to drive the ejector.

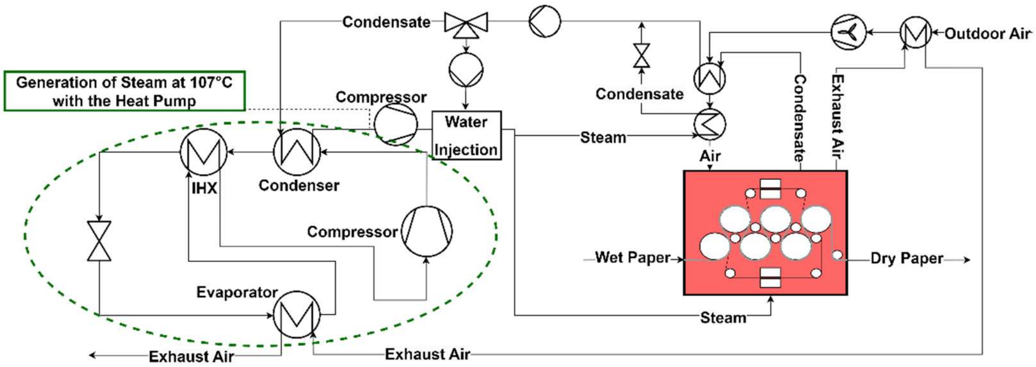

Figure 4. Proposed HTHP installation in the drying section of a packaging paper machine

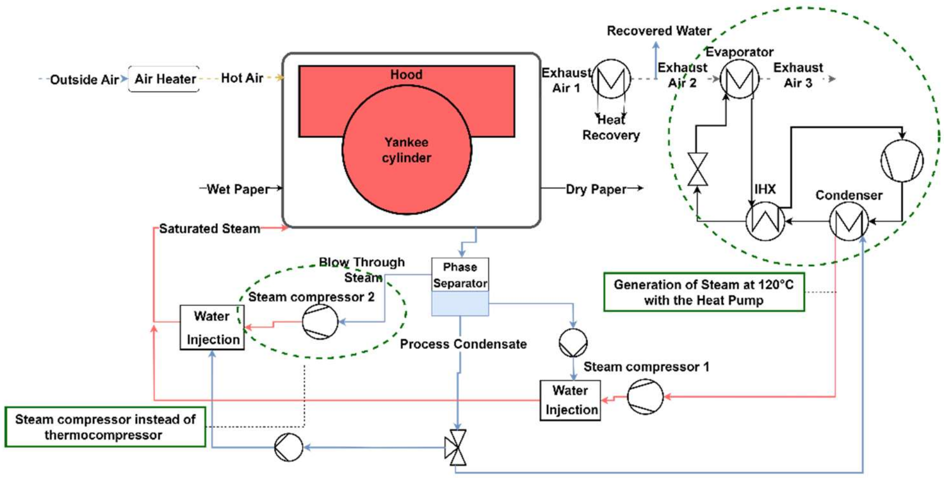

Figure 5. Proposed HTHP installation in the drying section of a tissue machine

3. Results and Discussion

In this chapter, the simulation results are presented. It begins with an explanation of the refrigerant selection process. This is followed by a thermodynamic assessment that quantifies COP, compression ratio, and energy consumption per ton of paper for each HTHP model across the different cases (packaging paper and tissue). Additionally, a sensitivity analysis explores how variations in exhaust air temperature influence heat pump efficiency. Finally, a pinch analysis estimates the maximum recoverable waste heat potential. Pinch analysis is conducted for a one case study (the packaging paper drying section) where detailed specifications of each heat exchanger were available which are important for the pinch analysis.

3.1. Refrigerant Selection

Since the heat pump needs to run at high temperatures to generate hot steam, all refrigerants with low critical temperatures and low pressures are excluded for the simulation. Subsequently, refrigerants with high GWP and ODP values are excluded. Table 1 lists the suitable refrigerants for HTHPs after filtering by various refrigerant properties.

Table 1. Suitable refrigerants for HTHP applications [15], [16].

Type	Refrigerant	$T_{critical}$ (°C)	$P_{critical}$ (bar)	ODP	GWP	SG*
HFO	R1336mzz(E)	137.7	31.5	0	18	A1
(Hydrofluoroolefin)	R1336mzz(Z)	171.3	29.0	0	2	A1
HCFO	R1224yd(Z)	155.5	33.3	0.00012	1	A1
(Hydrochlorofluoroolefin)	R1233zd(E)	166.5	36.2	0.00034	1	A1
HC (Hydrocarbon)	R600a (Iso-Butane)	134.7	36.6	0	3	A3
	R600 (Butane)	152.0	38.0	0	4	A3
	R601a (Iso-Pentane)	187.8	33.8	0	4	A3
	R601 (Pentane)	196.6	33.7	0	5	A3
Natural	R718 (Water)	373.9	220.6	0	0	A1
	R717 (Ammonia)	132.3	11.33	0	0	B2L

* Classification of the safety group (SG) is as follows: Toxicity: "A": Low toxicity, "B": Higher toxicity. Flammability: "1": Non-flammable, "2L": Lower flammability, "2": Flammable, "3": Highly flammable.

This analysis is limited to natural refrigerants and hydrocarbons. Synthetic refrigerants, which may provide better performance, are not considered due to potential future restrictions (PFAS bans).

3.2. HTHP Performance Evaluation

First, the thermodynamic framework used for the HTHP models is described as follows:
In this study, the HTHP cycle is analysed with the usual four refrigerant states (numbered position in HP cycles see Fig. 3):
1 → compressor inlet (vapour leaving the evaporator, 5 K superheat),
2 → compressor discharge,
3 → condenser exit (liquid with 7 K subcooling),
4 → evaporator inlet (after throttling).
Steady state, adiabatic components and negligible pressure losses in heat exchangers and piping are assumed. When present, an IHX links the 1-2 and 3-4 lines. In model c, the throttle valve is replaced by a turboexpander.
The assumptions in the calculation, such as isentropic efficiency and IHX effectiveness, as well as the main equations, are derived from the results of previous studies conducted by [13], [14], [17].

3.2.1. Component models:

- Condenser (heating duty):

$$\dot{Q}_{cond} = \dot{m}_{Ref}(h_2 - h_3) \quad (1)$$

With h_2 at compressor discharge and h_3 at the subcooled liquid outlet.

- Evaporator (source duty):

$$\dot{Q}_{eva} = \dot{m}_{Ref}(h_1 - h_4) \quad (2)$$

where h_1 is the superheated outlet and h_4 the post-expansion inlet.

- Expansion valve (isoenthalpic):

$$h_3 = h_4 \quad (3)$$

- Compressor:
  Isentropic efficiency: (in this study assumed 0.8)

$$\eta_{is} = \frac{h_{comp,out,is} - h_{comp,in}}{h_{comp,out} - h_{comp,in}} = \frac{h_{2s} - h_1}{h_2 - h_1} \quad (4)$$

and shaft/electrical power:

$$\dot{W}_{comp} = \dot{m}_{Ref}(h_2 - h_1) \quad (5)$$

Turboexpander (work recovered reduces the total power), see Fig. 3(c): The efficiency of the turboexpander in this study is taken to be 0.6.

$$\eta_{exp} = \frac{h_{exp,in} - h_{exp,out}}{h_{exp,in} - h_{exp,out,is}} = \frac{h_{3a} - h_4}{h_{3a} - h_{4,is}} \quad (6)$$

$$\dot{W}_{exp} = \dot{m}_{Ref}(h_4 - h_{3a}) \quad (7)$$

- IHX:

The IHX effectiveness is treated as a fixed parameter (in this study assumed 0.7), and it is calculated as follows: (cold stream: evaporator outlet, hot stream: condenser outlet (see Fig. 3(b)))

$$\varepsilon_{IHX} = \frac{T_{cold,out} - T_{cold,in}}{T_{hot,in} - T_{cold,out}} = \frac{T_4 - T_{4a}}{T_3 - T_4} \quad (8)$$

which sets the outlet temperatures of the hot and cold streams, subject to the specified 5 K superheat and 7 K subcooling bounds.

3.2.2. Performance metrics:

The heating COP of the HTHP cycle is (without including the steam compressions and pumps after the HTHP cycle):

$$COP_{HTHP} = \frac{\dot{Q}_{cond}}{\dot{W}_{HTHP}} \tag{9}$$

With expander replacing the valve:

$$\dot{W}_{HTHP} = \dot{W}_{comp} - \dot{W}_{exp} \tag{10}$$

To compare different models, the total COP accounts for auxiliaries:

- With steam compressor and condensate pump:

$$\dot{W}_{total} = \dot{W}_{HTHP} + \dot{W}_{steam,comp} + \dot{W}_{pump} \tag{11}$$

Then the total COP can be calculated as follows:

$$COP_{total} = \frac{\dot{Q}_{cond}}{\dot{W}_{total}} \tag{12}$$

This formulation maintains a compact model and enables fair comparison of HTHP layouts, with or without IHX, steam compression, and work recovery.

For the packaging paper and the tissue scenario, the results are as follows:

Table 2. Simulation results for the proposed HTHP; Refrigerant: **Water**

Parameter	Packaging Paper/model a	Packaging Paper/model b	Packaging Paper/model c	Tissue/model a	Tissue/model b	Tissue/model c
COP_{HTHP}	3.3	3.1	3.2	2.7	2.5	2.6
COP_{total}	2.6	2.5	2.5	1.8	1.7	1.7

Table 3. Simulation results for the proposed HTHP; Refrigerant: **R601a**

Parameter	Packaging Paper/model a	Packaging Paper/model b	Packaging Paper/model c	Tissue/model a	Tissue/model b	Tissue/model c
COP_{HTHP}	2.9	3.4	3.6	2	2.7	2.9
COP_{total}	2.3	2.7	2.8	1.4	1.8	1.9

Table 4. Simulation results for the proposed HTHP; Refrigerant: **R600**

Parameter	Packaging Paper/model a	Packaging Paper/model b	Packaging Paper/model c	Tissue/model a	Tissue/model b	Tissue/model c
COP_{HTHP}	2.7	3.3	3.5	1.8	2.5	2.7
COP_{total}	2.2	2.6	2.7	1.3	1.7	1.8

Table 5. Simulation results for the proposed HTHP; Refrigerant: **R717**

Parameter	Packaging Paper/model a	Packaging Paper/model b	Packaging Paper/model c	Tissue/model a	Tissue/model b	Tissue/model c
COP_{HTHP}	3	2.9	3.1	-	-	-
COP_{total}	2.4	2.3	2.4	-	-	-

The COP values (Tables 2-5) show clear advantages for the proposed HTHP options over the boiler reference, with performance depending on both configuration (models a-c) and working fluid. In the packaging case, COP_{HTHP} ranges from 2.7-3.6 and COP_{total} 2.2-2.8; the best values occur for R601a (model c, 3.6/2.8) and R600 (model c, 3.5/2.7), while water and R717 are close behind. In the tissue case, COPs are lower,1.8-2.9 (HTHP) and 1.3-1.9 (total), consistent with the higher effective temperature lifts, the strongest performer again is R601a (model c, 2.9/1.9), with water and R600 slightly below. The gap between COP_{HTHP} and COP_{total} reflects auxiliary power (steam compressors and pumps after HTHP). R717 was not evaluated for tissue in this study. The reason for this is the lower critical temperature and critical pressure of R717 compared to other selected refrigerants. For tissue, the condensation temperature in the HTHP condenser is higher than for packaging paper, while in this study, HTHP produces 107 °C saturated steam for packaging paper and 120 °C saturated steam for tissue. In the base scenario for packaging paper production, steam is generated using a natural gas boiler with an energy consumption of 885 kWhthermal/tpaper. For the baseline case in the tissue machine's drying section, the hot-air heating system consumes 660 kWhthermal/tpaper, while the natural gas boiler contributes an additional 540 kWhthermal/tpaper [10]. This study focuses on replacing only the natural gas boiler in the tissue machine with a HTHP, leaving the existing hot air heating system unchanged. Comparisons of energy consumption (Figs. 6-7) confirm these trends. In comparison to the gas-boiler baselines, the HTHP options cut specific energy in the packaging dryer to roughly 300-360 kWhelectrical/tpaper, and in the tissue dryer to about 210-240 kWhelectrical/tpaper. The lowest consumptions align with the highest COP cases (model c with R601a/R600), while water still delivers substantial reductions. Overall, selecting a suitable refrigerant and configuration is pivotal to maximise COP and minimise energy consumption in the paper drying section.

One observation from the results is, for water, the addition of an IHX (Model b) slightly reduces the COP compared to the basic configuration (Model a). Although the IHX increases liquid subcooling, it simultaneously increases suction superheat, leading to a higher compressor discharge temperature and higher compression work. Since the condenser heat duty is fixed by the process demand, the increase in compressor power dominates and results in a very small COP reduction. Replacing the throttling valve with a turboexpander (Model c) allows partial recovery of expansion work; however, for water this recovery is insufficient to compensate for the increased compression work caused by the IHX, so the COP remains slightly below that of Model a. In contrast, for other refrigerants like R601a, the IHX reduces throttling losses and the required refrigerant mass flow rate for a given condenser duty, which outweighs the suction superheat penalty and leads to a clear COP improvement. The addition of a turboexpander further reduces the net power input, resulting in the highest COP for Model c.

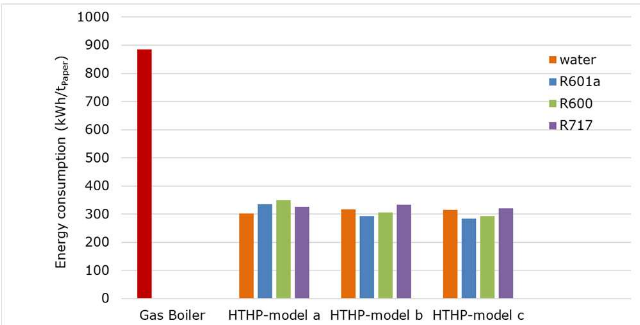

Figure 6. Specific energy use in the **Packaging** paper drying section (kWh/t $_{paper}$): baseline gas boiler vs. HTHP models a–c.

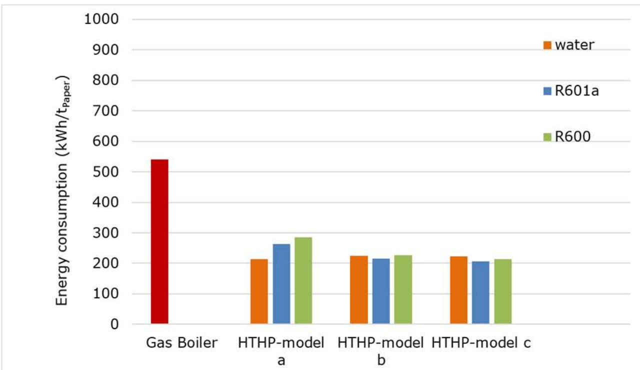

Figure 7. Specific energy use in the **Tissue** drying section (kWh/t $_{paper}$): baseline gas boiler vs. HTHP models a–c.

Although Figs. 6 and 7 show reduced energy consumption with HTHP integration, they do not indicate how much waste heat is recovered, how much remains unused, or where further heat-exchanger retrofits would be most effective. To address these aspects, the following section presents a pinch analysis of the paper machine with and without HTHP integration.

3.3. Pinch Analysis

This section links the HTHP to a system-level heat recovery analysis of the paper machine drying section. A pinch analysis of the base case without a heat pump is first performed, based on mass and energy balances normalized to 1 t/h of paper, to identify the pinch temperature, hot-utility demand, and available waste heat. The HTHP is then integrated into the heat-exchanger network, with the evaporator connected to low-temperature hood/exhaust-air streams and the condenser supplying heat to the steam network. The resulting composite curves quantify the recovered waste heat, the reduction in boiler duty, and the remaining unused waste heat potential. Pinch analysis provides thermodynamic targets for minimum heating and cooling by aggregating process streams into temperature, enthalpy composite curves (hot and cold) and locating the pinch point at the minimum approach temperature ΔT_{min}. From these, the grand composite curve (GCC) is constructed, using shifted temperatures, to visualize net heat deficits (above the pinch) and surpluses (below), and to guide utility targeting and technology placement [18]. Recent reviews and applications emphasize GCC-based targeting and its value for integrating electrified utilities such as heat pumps [11].

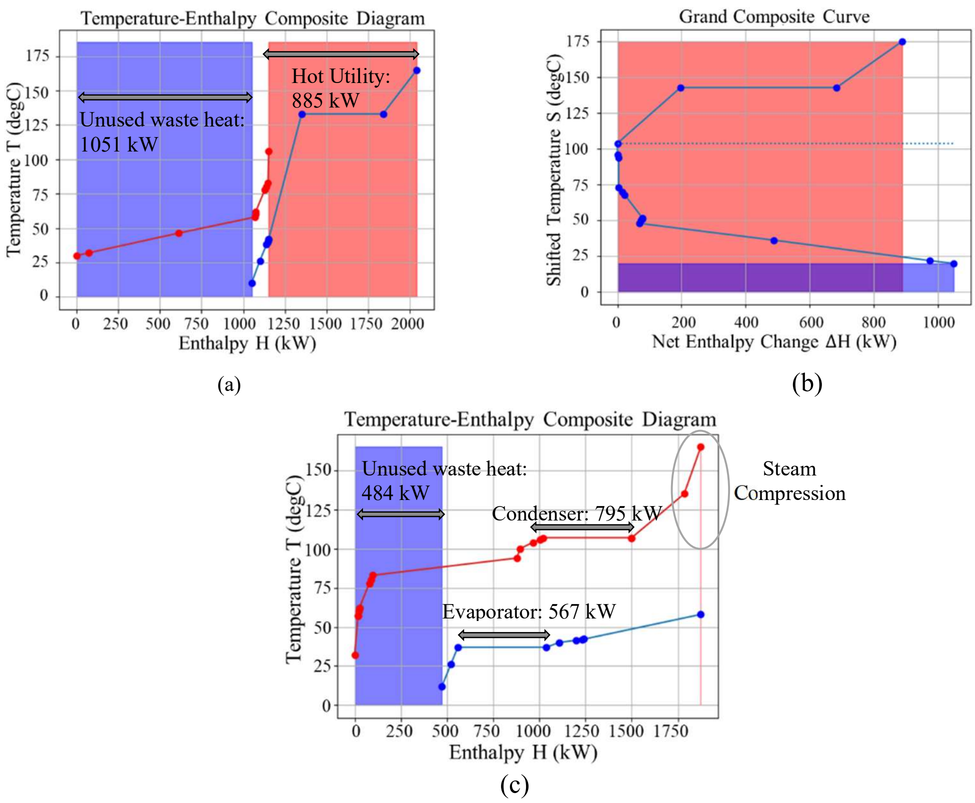

Figure 8. Pinch analysis results (enthalpy in kW/t_{paper}): (a) Temperature-enthalpy composite diagram: Case study without heat pump; (b) Grand-composite curve: Case study without heat pump; (c) Temperature-enthalpy composite diagram: Case study with heat pump and steam compression (see Fig. 4)

In this study, only the packaging paper scenario's dryer section is used for the pinch analysis, since detailed heat exchanger data are necessary and available only from the packaging paper mill. The Python module, PyPinch [19] is used to display the results of the pinch analysis. Targets for hot and cold utilities are obtained and opportunities for heat recovery are outlined. The resulting diagrams are used to compare conventional operation (without a heat pump) with an electrified case in which a HTHP is integrated. A minimum temperature difference of 20 K is used for the calculations. It should be mentioned that all mass and energy balances used for the pinch analysis have been normalized to a production rate of 1 ton of paper per hour. Consequently, the hot utility and waste heat quantities shown in the composite curves are given per ton of paper. In the base case (without HTHP), the temperature-enthalpy composite diagram (Fig. 8(a)) shows a significant demand for hot energy above the pinch point; the GCC (Fig. 8(b)) also shows a wide range with heat deficiency. When HTHP is integrated (second proposed model (Fig. 3 model b) with R601a as refrigerant), configured with an IHX, post-condenser steam compression to provide supply pressure/temperature, and water injection to prevent overheating, the updated composite temperature-enthalpy plot (Fig. 8(c)) removes the external heat utilization bar for the dryer section and reduces cold utilization output. In fact, the HTHP bridges the pinch point and converts the exhaust air waste heat (below the pinch point) into steam demand (above), which is consistent with the recommended placement rules for heat pump integration from the GCC analysis. The results indicate a complete elimination of hot utility (thermal energy demand), decreasing from 885 kW (See Fig. 1: Thermal energy = $\dot{Q}_{Boiler}$) to 0 kW, but adding the electrical energy demand of 293 kWh/t paper for the compressors, alongside a 54% reduction in unused waste heat, from 1051 kW to 484 kW. This shift is accompanied by a transition from thermal to electrical energy demand, primarily due to the integration of a heat pump and steam compressor.

4. Conclusions

This work evaluates HTHP integration for two representative drying systems; cylinder drying for packaging paper and Yankee-cylinder drying for tissue, and benchmarks them against a natural-gas boiler. Python models were developed to compare working fluids and practical layouts (IHX, turboexpander, steam compression, and water injection for steam temperature control), and a pinch study was used to set integration targets on the packaging drying process. Across both cases, the HTHP options outperform the boiler reference. In packaging paper scenario, the best configuration R601a with IHX + turboexpander + steam compressor + water injection, achieves COP_{total} =2.8 and cuts the dryers energy use by ~68% relative to the boiler. In tissue case, the same configuration delivers COP_{total} around 1.9 and a ~61.7% reduction. Pinch analysis of the packaging paper dryer confirms the integration logic: the HTHP bridges the pinch, upgrading exhaust-air heat below the pinch to steam demand above it. With ΔT_{min} = 20 K, the hot utility requirement falls from 885 kW to 0 kW, and unused waste heat drops by 54% (1051 → 484 kW). These objectives convert the thermal load into an electrical one (thermal energy consumption (base case: 885 kWh/tpaper) to electrical energy consumption (293 kWh/t paper)), in line with the measured COP gains, and provide clear placement rules for retrofits (source on the hood/exhaust air side, sink in the steam network with post-condenser compression).

Overall, the results demonstrate that HTHPs can substantially improve dryer-section efficiency and enable deep fuel switching in papermaking when source/sink conditions and cycle design are aligned. Future work should (i) validate these findings with pilot data (ii) extend pinch and control design to the full machine (hood, breakers, condensate return); (iii) assess safety and permitting for hydrocarbon refrigerants; and (iv) quantify CO_2 outcomes under local grid-carbon intensities and electricity/ fuel price scenarios; and (v) check reliability of complex HTHP configurations during on-machine implementation.

Nomenclature

Category	Symbol / Acronym	Description	Unit
Latin symbols	h	Specific enthalpy	J/kg
	$\dot{m}$	Mass flow rate	kg/s
	Q	Heat transfer rate	W
	$\dot{w}$	Power	W
Greek symbols	η	Efficiency	-
	ε	Internal heat exchanger effectiveness	-
Subscripts	comp	Compressor	-
	con	Condenser	-
	eva	Evaporator	-
	exp	Expander	-
	is	Isentropic	-
	Ref	Refrigerant	-

Acronyms	COP	Coefficient of performance	-
	GWP	Global warming potential	-
	HTHP	High temperature heat pump	-
	IHX	Internal Heat exchanger	-
	ODP	Ozone depletion potential	-
	PFAS	Per- and poly- fluoroalkyl substances	-

Acknowledgements

This work has been conducted as part of the research project Forschungscluster Modellfabrik Papier (FOMOP)" and has been supported by the German Federal Ministry of Research, Technology and Space (BMFTR) (funding reference number: 03STG011F).

References

[1] EHPA and Cepi, "THROUGH PUMPS TO PULP: GREENING THE PAPER INDUSTRY'S HEAT," 2023. Accessed: Oct. 01, 2025. [Online]. Available: https://www.cepi.org/wp-content/uploads/2023/02/Cepi-x-EHPA.pdf

[2] Confederation of European Paper Industries, "Strengthening the global competitiveness of Europe's circularity and bioeconomy sector in the EU ETS." Cepi, 2025. Accessed: Oct. 01, 2025. [Online]. Available: https://www.cepi.org/cepi-position-paper-on-the-2026-ets-review/

[3] J. Gollasch, M. Kriese, J. Siegel, N. Kabat, and J. Walden, "Numerical investigation of a heat pump demonstrator for partial electrification of the steam supply for paper drying," *Appl. Therm. Eng.*, p. 126941, 2025.

[4] Accessed: Oct. 01, 2025. [Online]. Available: https://modellfabrikpapier.de/

[5] X. Ma, Y. Du, T. Zhao, T. Zhu, B. Lei, and Y. Wu, "A comprehensive review of compression high-temperature heat pump steam system: Status and trend," *Int. J. Refrig.*, vol. 164, pp. 218–242, 2024.

[6] M. Pellegrini, A. Guzzini, and C. Saccani, "Feasibility study for the application of a high-temperature heat pump in the pulp and paper industry: an Italian case study," in *14th IEA Heat Pump Conference, Chicago, United States*, 2023.

[7] J. Jeßberger, C. Arpagaus, F. Heberle, L. Brendel, S. Bertsch, and D. Brüggemann, "Experimental investigations of upscaling effects of high-temperature heat pumps with R1233zd (E)," *Int. J. Refrig.*, vol. 164, pp. 243–256, 2024.

[8] J. Rosenow, C. Arpagaus, S. Lechtenböhmer, S. Oxenaar, and E. Pusceddu, "The heat is on: Policy solutions for industrial electrification," *Energy Res. Soc. Sci.*, vol. 127, p. 104227, 2025.

[9] C. Mateu-Royo, C. Arpagaus, A. Mota-Babiloni, J. Navarro-Esbrí, and S. S. Bertsch, "Advanced high temperature heat pump configurations using low GWP refrigerants for industrial waste heat recovery: A comprehensive study," *Energy Convers. Manag.*, vol. 229, p. 113752, 2021.

[10] A. Ciambellotti, G. F. Frate, A. Baccioli, and U. Desideri, "High-Temperature Heat Pumps for Electrification and Cost-Effective Decarbonization in the Tissue Paper Industry," *Energies*, vol. 17, no. 17, p. 4335, 2024.

[11] C. Arpagaus *et al.*, "Integration of High-Temperature Heat Pumps in Swiss Industrial Processes (HTHP-CH)," in *14th IEA Heat Pump Conference*, 2023.

[12] V. Wilk, S. B. Knöttner, G. Drexler-Schmid, and T. Barz, "Superheated steam drying for paper production: Process efficiency assessment," in *Proceedings of ECOS 2023: 36th International Conference on Efficiency, Cost, Optimization, Simulation and Environmental Impact of Energy Systems*, 2023, pp. 1411–1421.

[13] B. Luo and P. Zou, "Performance analysis of different single stage advanced vapor compression cycles and refrigerants for high temperature heat pumps," *Int. J. Refrig.*, vol. 104, pp. 246–258, 2019.

[14] B. Zhan *et al.*, "Experimental investigation on a semi-open air cycle heat pump system equipped with booster turbo-expander," *Energy Convers. Manag.*, vol. 318, p. 118889, 2024.

[15] T. El Samad, A. Żabnieńska-Góra, H. Jouhara, and A. I. Sayma, "A review of compressors for high temperature heat pumps," *Therm. Sci. Eng. Prog.*, p. 102603, 2024.

[16] Y. Dong and R. Wang, "When and how to use cascade high temperature heat pump—Its multi-criteria evaluation," *Energy Convers. Manag.*, vol. 309, p. 118435, 2024.

[17] S. M. Hosseinnia, L. Amiri, H. Nesreddine, D. Monney, and S. Poncet, "Thermodynamic analysis of high temperature cascade heat pump with R718 (high stage) and six different low-GWP refrigerants (low stage)," *Case Stud. Therm. Eng.*, vol. 53, p. 103812, 2024.

[18] T. Yuan and Y. Mao, "A review of pinch analysis techniques and extended application in power systems," *Renew. Sustain. Energy Rev.*, vol. 202, p. 114684, 2024.

[19] A. Nicusan, GitHub. Accessed: Oct. 01, 2025. [Online]. Available: https://github.com/anicusan/PyPinch